

## The Entraining Hydraulic Jump

By D. L. WILKINSON, B.E., GRAD.I.E.AUST. and I. R. WOOD, PH.D., M.I.E.AUST.\*

**Summary.**—This paper presents the results of a study of the zone of flow establishment of a steady two-dimensional horizontal density current. It is shown that the form of jump in this zone depends markedly on the tailwater conditions and for a jump that is not flooded two distinct types exist. These have downstream Froude numbers of 1.0 and of 0.5 respectively. Detailed measurements are presented for the jump with a downstream Froude number of 0.5.

### LIST OF SYMBOLS

$D$	Depth of flume.
$F$	Froude number.
$g$	Gravitational acceleration.
$K$	Entrainment parameter.
$M$	Flow force.
$Q$	Flow.
$Re$	Reynolds number.
$r$	Conjugate depth ratio.
$S_h$	Density correction factor.
$S_m$	Velocity correction factor.
$u$	Local velocity.
$u'$	Characteristic velocity.
$y$	Local depth.
$y'$	Characteristic depth = depth to interface.
$y_{1c}$	Critical depth of upstream discharge.
$Y$	Dimensionless depth.
$\rho$	Density of ambient fluid.
$\Delta\rho$	Local density deficit.
$\Delta\rho'$	Characteristic density deficit.
$\theta$	Flow force loss ratio.
$\nu$	Kinematic viscosity.
1 and 2	Subscripts referring to the upstream and downstream sections respectively.

### 1.—INTRODUCTION

The flow under investigation is that of a hydraulic jump in a two-layer system. The fluids are of different densities and are miscible so that there may be mixing of the two layers in the turbulent region of the jump. This type of situation is found whenever a fluid is discharged from an outlet under a horizontal boundary into a fluid of greater density, or over a horizontal boundary into a fluid of lesser density. An important example of a flow of this type is the discharge of hot water into a power station cooling pond.

For the case under analysis the Boussinesq assumption is made. That is, it is assumed that the density difference between the moving layer and the ambient fluid is so small that variations in the inertial forces can be neglected. The analysis of the entraining jump is very similar to that for a normal open channel jump, except that the equation of continuity is replaced by the equation of continuity of density excess or deficit and that an extra variable, the quantity of entrained fluid, is involved. Initially then, the equation for the conservation of the sum of horizontal momentum flux and pressure force per unit span is examined (Ref. 1). This quantity will be referred to as the flow force after Benjamin (1962, Ref. 2). There are insufficient equations available to obtain a complete solution and for any value of downstream depth there are two downstream discharges which will satisfy the flow force equation. However, from a consideration of this equation the upper and lower bounds of the possible discharges are obtained.

### 2.—THEORY

#### 2.1 The Flow Force Equation:

Consider a fluid flowing as in Fig. 1. Let the depth  $y'$  of the density current be defined by the distance between the visual interface and the free surface or roof. The characteristic velocity  $u'$  can then be defined by

$$u' = \frac{1}{y'} \int_0^{y'} u \, dy$$

The flow force  $M$  at a section may be written as

$$M = \int_0^D \int_0^{y'} \Delta\rho g \, dy \, dy + \int_0^D \rho u^2 \, dy$$

It is convenient to define  $\Delta\rho'$ ,  $S_m$ , and  $S_h$  by

$$\Delta\rho' = \frac{1}{u' y'} \int_0^{y'} u \, \Delta\rho \, dy$$

$$S_m = \frac{1}{u'^2 y'} \int_0^{y'} u^2 \, dy$$

$$S_h = \frac{2}{\Delta\rho' y'^2} \int_0^D \int_0^{y'} \Delta\rho \, dy \, dy$$

where  $S_m$  and  $S_h$  are dimensionless velocity and density correction factors which depend on the velocity and density distributions. For the case where the velocity and density distributions are rectangular  $S_m$  and  $S_h$  equal unity. Substituting the above into the expression for the flow force the following equation is obtained:

$$M = S_m \rho u'^2 y' + \frac{S_h}{2} \Delta\rho' g y'^2$$

or in terms of the total flow

$$Q = \int_0^D u \, dy = u' y'$$

$$M = S_m \rho \frac{Q^2}{y'} + \frac{S_h}{2} \Delta\rho' g y'^2 \quad \dots\dots\dots(1)$$

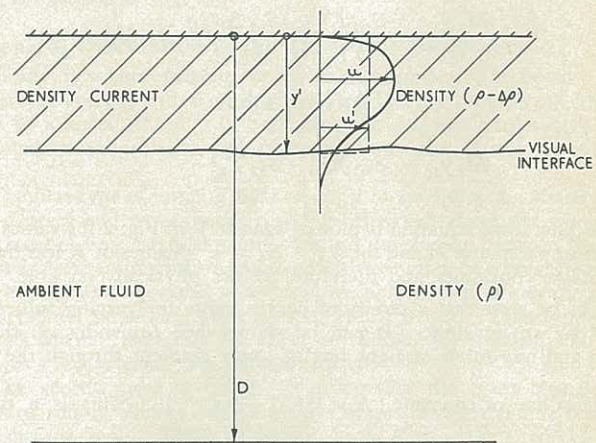


Fig. 1.—Definition Sketch of Density Current.

It is now convenient to define the inflow volumetric discharge and density difference as the characteristic discharge and density difference and to write Eq. (1) in a non-dimensional form. A characteristic depth does not need to be defined as it may be obtained from an arrangement of the already defined variables, i.e.,

$$y_{1c} = \left[ \frac{\rho Q_1^2}{\Delta\rho' g} \right]^{1/3}$$

It is worth noting that  $y_{1c}$  is the critical flow depth defined from the Froude number equals 1.0 and since the flux of density difference is a constant ( $Q \frac{\Delta\rho'}{\rho} g = \text{constant}$ ),  $y_{1c}$  is proportional to  $Q_1$ . Now let the new variables  $K$  and  $Y$  be defined by

$$K = \frac{Q_2}{Q_1} = \frac{y_{2c}}{y_{1c}}$$

$$Y = \frac{y'_2}{y_{1c}}$$

\*Paper No. 2591, presented at the Third Australasian Conference on Hydraulics and Fluid Mechanics held in Sydney from 25th to 29th November, 1968.

Mr. Wilkinson is a Teaching Fellow and Dr. Wood a Senior Lecturer with the School of Civil Engineering, University of New South Wales.







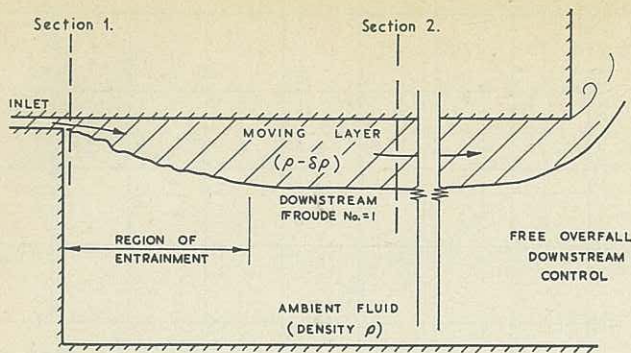


Fig. 4.—Type I Entraining Hydraulic Jump.

ambient fluid made up of a salt (NaCl) solution. In the former case the density deficit was determined by measuring the temperatures of the inflowing and ambient fluids and in the latter case samples of the salt solution were analysed. Both the experiments and the theoretical work showed the heat losses through the boundaries were negligible.

Density measurements within the steady uniform thermal density current downstream of the jump were made using a calibrated copper-constantin thermocouple probe wired to a micro-voltmeter. The reference junction was placed in the inlet slot and the measuring junction was lowered through the roof of the working section into the density current. When a freshwater current with an ambient saline fluid of the same temperature and density was used, measurements were made by withdrawing 10-ml. samples through a hypodermic tube. The density of the samples was then determined using a calibrated conductivity meter.

For the thermal density current, velocity measurements were obtained from photographs of hydrogen bubbles pulsed from a 0.002-in. dia. platinum wire which was placed in the vertical plane in the centre of the density current.

From these measurements the inlet and downstream Froude numbers, the ratio of the downstream volume flow to the inlet volume flow and the conjugate depth ratio ( $r$ ) were obtained. It is important to note that all the downstream measurements were made at positions where the slope of the interface of the density current was zero.

The downstream Froude numbers ( $F_2$ ) were obtained in different ways in two of the series of tests.

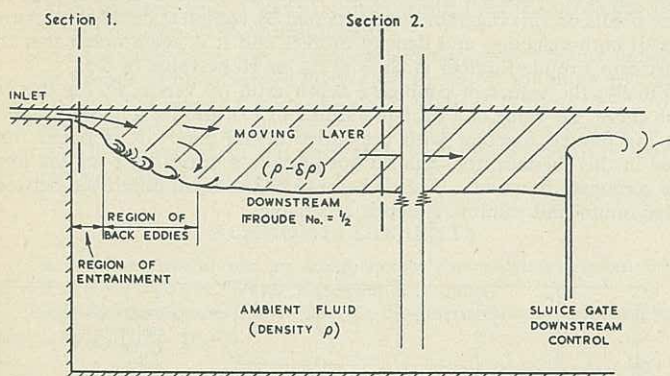


Fig. 5.—Type II Entraining Hydraulic Jump.

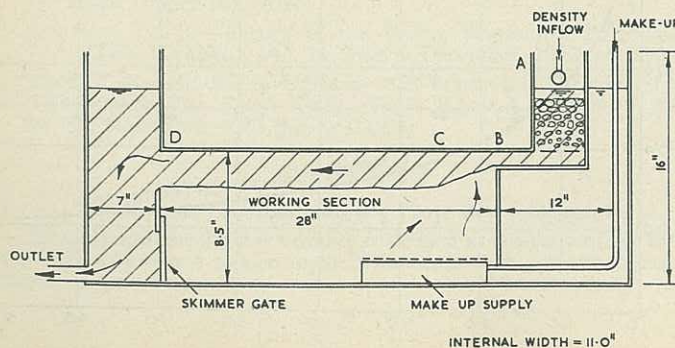


Fig. 6.—Schematic Diagram of Experimental Equipment.

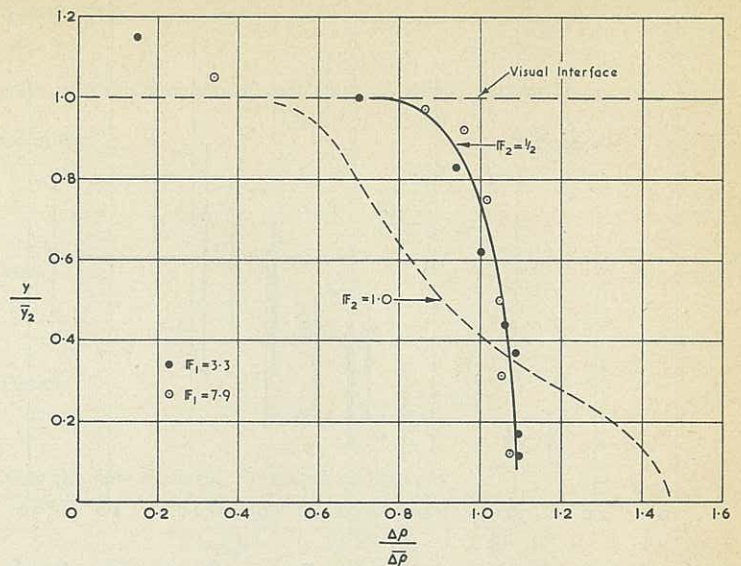


Fig. 7.—Dimensionless Density Profiles.

Firstly, measured values of  $K$  and  $r$  were combined with dimensionless  $S_m$  values obtained from hydrogen bubble photographs. Use was made of the continuity relation between upstream and downstream sections and the density correction factor  $S_h$  was assumed to be 1.00 (Fig. 7).

Secondly,  $F_2$  values were determined by direct measurement of  $\int_0^D u^2 dy$  from the bubble photographs, measurement of the density deficit and depth of the downstream flow.

The results obtained by both methods were in close agreement and are shown plotted in Fig. 11.

### 3.2 General Description of the Types of Flow Observed:

Firstly, it is appropriate to note that there appeared to be no difference between the current with a density deficit caused by thermal effect and that caused by a deficit of salt. In both cases experiments have shown that the establishment zone of the density current was one of two types (Figs. 4 and 5).

The first type of jump (I) had an angle of spread of the visual interface of 15 degrees and entrainment could be observed along the whole length of the zone of flow establishment. Indeed the surface between the density current and the ambient fluid appeared similar to that of a normal entraining jet. Entrainment appeared to become negligibly small when the tailwater depth reached something close to the critical depth. This type of jump occurred when (a) starting the flow, or suddenly increasing the flow, or when (b) a free overfall was maintained.

The second type of jump (II) resembled the open channel jump. Backward rolling surface eddies were observed along the interface of the establishment zone. These relatively large, slow-moving eddies covered the high-velocity fluid and effectively prevented the density current from entraining the ambient fluid. Thus the effective entrainment was restricted to a region near the outlet where these large surface eddies were absent. In this region the surface of the jump appeared the same as that of a type (I) jump. The slope of the type (II) jump was steeper than the type (I) and had a slope of the visual interface of 20 degrees. It was important to note that in every case a type (I) jump first formed and then the downstream conditions determined whether the jump remained of this type or changed into a type (II) jump.

Detailed measurements showed that type (I) jumps result in a markedly non-rectangular density distribution in the steady layer downstream (Fig. 7). This implied that the turbulence in the jump was insufficient to promote the complete mixing of the entrained fluid. In the second type of jump where the entrainment was confined to the beginning of the establishment zone, the turbulence in the establishment zone permitted the complete mixing of the entrained fluid, and the resulting downstream density distribution was nearly rectangular (Fig. 7). Thus the interface was sharp and accurate measurements of the downstream depth were possible.

Velocity distributions for the type (II) jump were dependent on the inlet Froude number. This is shown in Fig. 8 where the velocity correction factor has been plotted against the inlet Froude number. The Reynolds numbers of the experimental downstream flows were relatively small (400 to 1,100) and it is thought that this variation might be due to a Reynolds number effect.



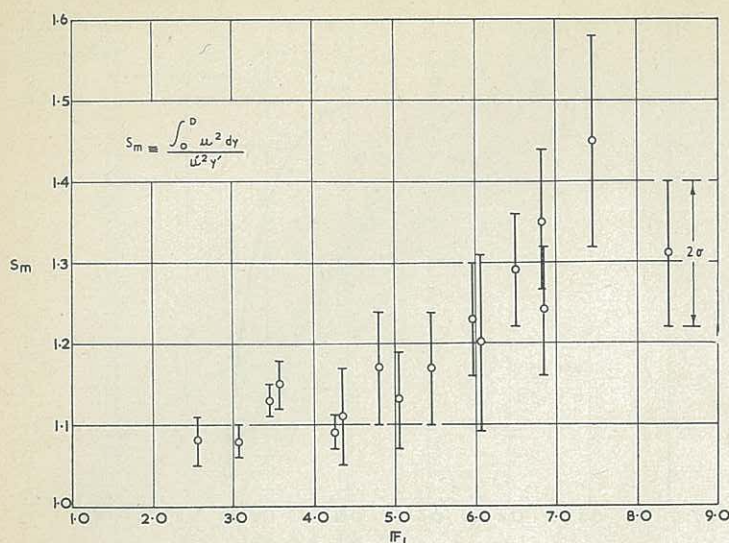


Fig. 8.—Velocity Distribution Correction Factors ( $S_m$ ) vs. Inlet Froude Number.

The Reynolds number ( $Re$ ) was defined as  $Re = \frac{u' y'}{\nu}$

Finally, it is worth noting that during all the experiments the tailwater conditions were not critically controlled and it appeared that the downstream Froude number of 0.5 was oddly insensitive to a range of tailwater conditions. Indeed it is curious, for this implies that the depth downstream of the jump was always the maximum possible.

### 3.3 Quantitative Deduction from the Experiments with the Type II Jump:

The quantitative measurements were directed towards the investigation of type (II) jumps and it is not proposed to discuss the first type of jump in detail. However it is worth noting that measurements of unsteady flows (Ref. 3) imply that the downstream Froude number for the type (I) jump is approximately 1.0.

It was appropriate to plot the experimental values of  $Y_2$  and  $K$  on the flow force diagram. When this was done, it was noted that for type (II) jumps all the points were close to the envelope. The ratio of the depths, however, could not be measured as accurately as could the amount of entrainment. Hence, a considerably more sensitive check on the closeness of the experimental points to the envelope could be obtained using the measurements of entrainment. Assuming conservation of momentum the equation of the envelope may be written as

$$K S_m^{2/3} S_h^{1/3} = \frac{2 F_1^2 + 1}{3 (2 F_1)^{4/3}}$$

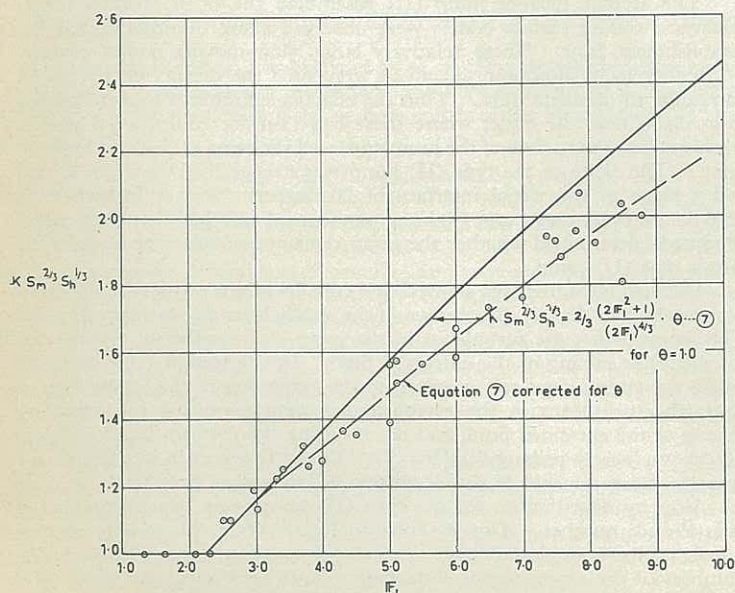


Fig. 9.—Entrainment Parameter vs. Inlet Froude Number.

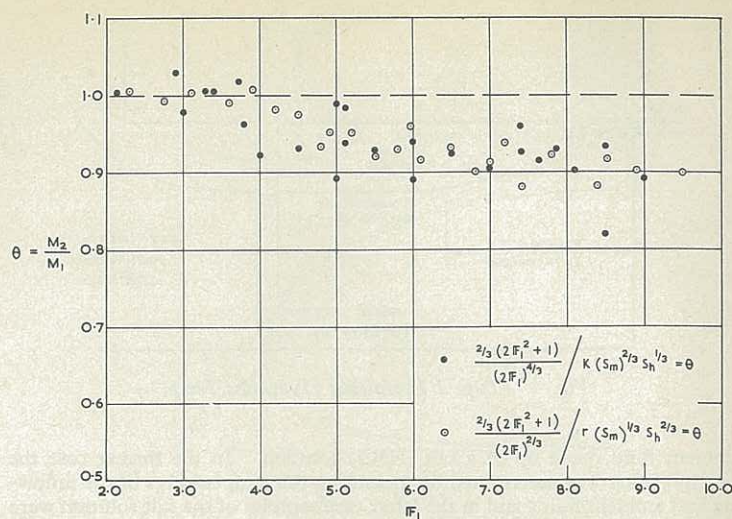


Fig. 10.—Momentum Loss Between Sections (1) and (2).

This equation is derived in Appendix II and has been plotted in Fig. 9. Thus if the points were on the envelope this curve would enable values of  $K$  to be predicted. The experimental values of  $K S_m^{2/3} S_h^{1/3}$  are also plotted on Fig. 9 and it is noted that all the points are close to the envelope curve. Indeed if a correction is made for the momentum loss caused by boundary friction in the zone of flow establishment (Fig. 10) the agreement is remarkable. This boundary friction loss obtained experimentally was close to that calculated assuming a laminar boundary layer.

It is noteworthy that this plot implies that there was no entrainment in the jump if the inlet Froude number was less than 2.3. This is in accord with the flow force diagram. Indeed it can be seen in Fig. 2 that in order to reach the envelope the conjugate function must follow the non-entraining  $K = 1.0$  curve until a Froude number of 2.25 is reached. At this point the conjugate depth curve for a non-entraining jump is tangential to the envelope. Further it was observed in the experiments that when the inlet Froude number was less than 2.3 the eddies that were blanketing the high-velocity current had advanced back to the inlet and entrainment was completely inhibited.

A further confirmation was obtained by plotting the downstream Froude number versus the inlet Froude number. This is done in Fig. 11. All the points on this diagram were obtained by complete detailed measurements of both velocities and density profiles and it is again noted that the downstream Froude number is close to its envelope value of 0.5.

Finally, the values of conjugate depth ratio ( $r$ ) versus  $F_1$  for the envelope curve, the value of a Froude number of 1.0, and for a non-entraining curve are plotted together with the experimental data. It is noted that, plotted in this manner, the data do not provide a critical test for the form of the conjugate function. This is because of the small difference between the maximum and minimum depth attainable.

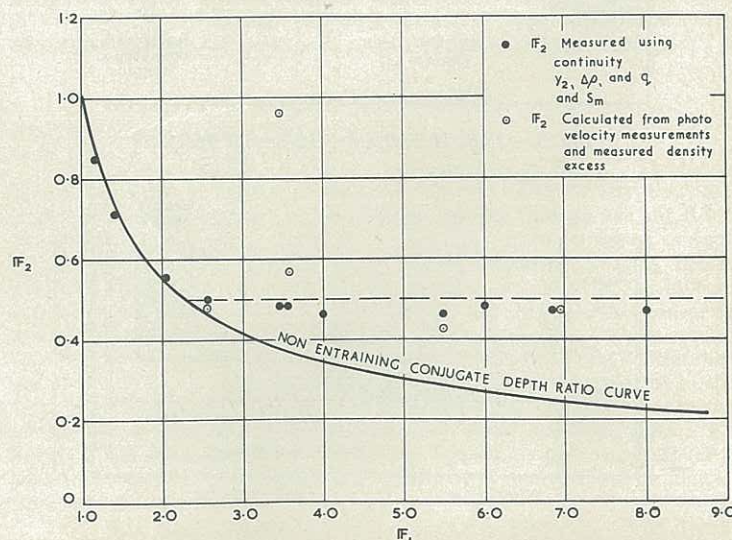


Fig. 11.—Downstream Froude Number vs. Upstream Froude Number.



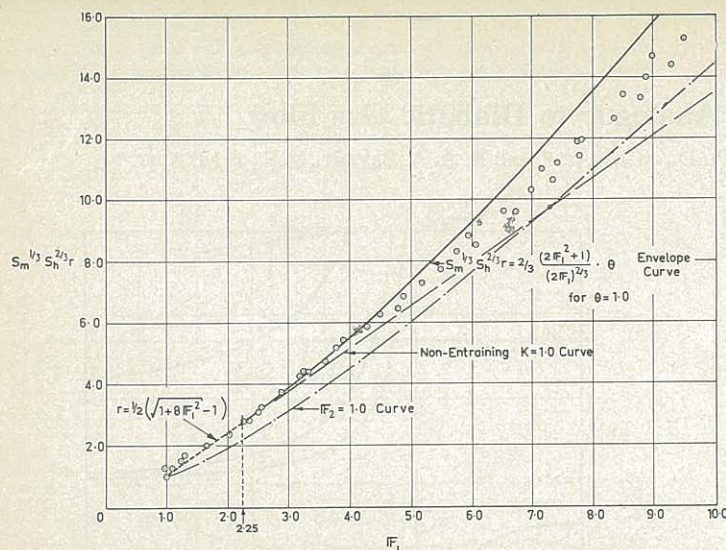


Fig. 12.—Conjugate Depth Ratio vs. Inlet Froude Number.

In view of the fact that the depth of fluid at the outflow sluice could be varied considerably, it seems significant that no downstream Froude numbers intermediate between 0.5 and 1.0 were obtained. It was expected that the entrainment in the jump could have been controlled by setting a tailwater depth. This was not the case and if the tailwater was set beneath the envelope depth the flow between the jump and the control would be steady but non-uniform. The Froude number immediately downstream of the jump still had the value of 0.5. If the tailwater was set higher than the envelope depth the jump would flood out as expected.

It therefore appears that in these series of experiments only two stable jumps existed. These stable jumps had downstream Froude numbers of 0.5 or 1.0 depending on the tailwater conditions.

### CONCLUSIONS

The significant conclusions from this work are:

- (1) Two types of entraining hydraulic jump are possible; and,
- (2) The determining factor for each is the tailwater control depth.

If the tailwater control was at critical depth then the conjugate depth for the jump was forced to critical depth.

If the tailwater depth was subcritical and the jump remains unflooded then the Froude number immediately downstream of the jump was found to be 0.5 over the range of inlet Froude numbers 2.25 to 8. No entrainment was observed for Froude numbers less than 2.25 for the second type of jump. The entrainment was such that the conjugate depth of the type (II) jump was always a maximum.

### ACKNOWLEDGMENTS

The authors would like to acknowledge the assistance given by the members of staff of the Water Research Laboratory.

Particular thanks are due to Mr. G. S. Harris who contributed to the initial stages of this study.

### References

1. WOOD, I. R.—Horizontal Two-Dimensional Density Current. *Proc. A.S.C.E., Jour. Hydraulics Div.*, Vol. 93, No. HY2, March, 1967, pp. 35-42, (Paper No. 5139).
2. BENJAMIN, T. B.—Theory of the Vortex Breakdown Phenomenon. *Jour. Fluid Mechanics*, Vol. 14, Part 4, December, 1962, pp. 593-629.
3. WOOD, I. R.—Studies in Unsteady Self-Preserving Turbulent Flows. *University of New South Wales, Water Research Laboratory, Report No. 81*, November, 1965, pp. 96-118.

### APPENDIX I

#### The Froude Number and the Flow Force Diagram

In this paper the Froude number is defined as the ratio of the inertial force integrated over a section to the hydrostatic force integrated over the section. This becomes

$$\left[ \frac{S_m Q^2}{S_h \frac{\Delta \rho'}{\rho} g y'^3} \right]^{1/2}$$

Substituting,

$$y' = Y y_{1c}$$

$$Q = K Q_1$$

and using the equation of continuity of density excess, i.e.,

$$Q_1 \Delta \rho'_1 = Q \Delta \rho'$$

we obtain

$$F = \left[ \frac{S_m K^3}{S_h Y^3} \cdot \frac{Q_1^2}{\frac{\Delta \rho'_1}{\rho} g y_{1c}^3} \right]^{1/2} \dots \dots \dots (3)$$

but

$$\frac{Q_1^2}{\frac{\Delta \rho'_1}{\rho} g y_{1c}^3} = 1$$

Hence

$$F = \left[ \frac{S_m K^3}{S_h Y^3} \right]^{1/2}$$

Now the flow force Eq. (2) may be written as

$$\frac{M y_{1c}}{\rho Q_1^2} = \left[ \frac{2 S_m K^3}{S_h Y^3} + 1 \right] \frac{S_h Y^2}{2 K}$$

Substituting for  $F$  we have

$$\frac{M y_{1c}}{\rho Q_1^2} = \left[ \frac{2 F^2 + 1}{2 F^{2/3}} \right] S_h^{2/3} S_m^{1/3} Y \dots \dots \dots (4)$$

Hence if  $F$ ,  $S_m$  and  $S_h$  are constants there is a linear relationship between  $M$  and  $Y$ .

Using this equation it can be shown that for a given  $M$ ,  $Y$  is a maximum when the Froude number downstream equals 0.5.

### APPENDIX II

#### The Variation of the Discharge Ratio ( $K$ ) and the Conjugate Depth Ratio ( $r$ ) on the Envelope of the Flow Force Diagram

If for the upstream flow  $S_m$  and  $S_h$  equal 1.0 then the flow force Eq. (2) may be written as

$$\frac{M_1 y_{1c}}{\rho Q_1^2} = \left[ \frac{1}{Y_1} + \frac{Y_1^2}{2} \right]; \quad \frac{M_2 y_{1c}}{\rho Q_1^2} = \frac{S_{m2} K^2}{Y_2} + \frac{S_{h2} Y_2^2}{2 K}$$

$\theta$ , the ratio of the flow force at Section 2 to the flow force at Section 1 may be written as

$$\theta = \frac{\frac{S_{m2} K^2}{Y_2} + \frac{S_{h2} Y_2^2}{2 K}}{\frac{1}{Y_1} + \frac{Y_1^2}{2}} = \frac{M_2}{M_1} \dots \dots \dots (5)$$

On the envelope

$$F_2^2 = \frac{S_{m2} K^3}{S_{h2} Y_2^3} = \frac{1}{4}$$

and from Eq. (4)

$$F_1 = \left[ \frac{Q_1^2}{\frac{\Delta \rho'_1}{\rho} g y_{1c}^3} \right]^{1/2} = \left[ \frac{y_{1c}}{y'_1} \right]^{3/2} = \left[ \frac{1}{Y_1} \right]^{3/2} \dots \dots \dots (6)$$

Substituting the above into the equation for  $\theta$  we get after some manipulation,

$$K = \frac{2}{3} \frac{\theta}{(S_{m2})^{2/3}} \frac{1}{(S_{h2})^{1/3}} \cdot \frac{2 F_1^2 + 1}{(2 F_1^2)^{4/3}} \dots \dots \dots (7)$$

and this is the relationship between the discharge ratio  $K$  and the Froude number on the envelope of the flow force diagram. Similarly if we use

$$r = \frac{y'_2}{y'_1} = \frac{Y_2}{Y_1} = (F_1)^{2/3} Y_2 \dots \dots \dots (8)$$

where  $r$  is the conjugate depth ratio, we get for the relationship on the envelope

$$r = \frac{2}{3} \frac{\theta}{(S_{m2})^{1/3}} \frac{1}{(S_{h2})^{2/3}} \cdot \frac{2 F_1^2 + 1}{(2 F_1^2)^{2/3}}$$